NASA Technical Paper 3273

August 1992

Influence of Mass Moment of Inertia on Normal Modes of Preloaded Solar Array Mast

Sasan C. Armand
and Paul Lin

NASA

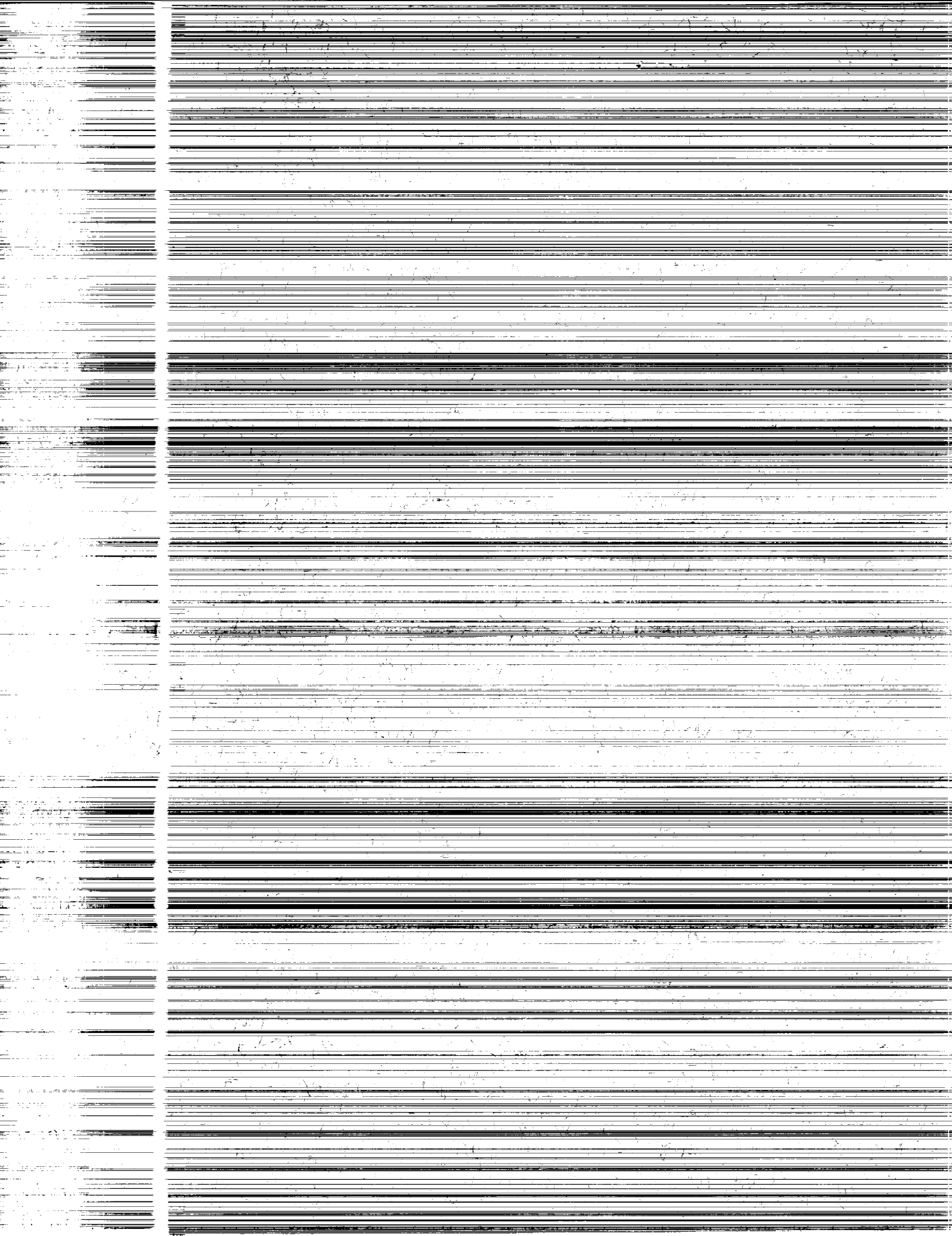

NASA Technical Paper 3273

1992

Influence of Mass Moment of Inertia on Normal Modes of Preloaded Solar Array Mast

Sasan C. Armand
Lewis Research Center
Cleveland, Ohio

Paul Lin
Cleveland State University
Cleveland, Ohio

National Aeronautics and Space Administration

Office of Management

Scientific and Technical Information Program

Summary

Earth-orbiting spacecraft often contain solar arrays or antennas supported by a preloaded mast. Because of weight and cost considerations, the structures supporting the spacecraft appendages are extremely light and flexible; therefore, it is vital to investigate the influence of all physical and structural parameters that may influence the dynamic behavior of the overall structure. The study reported in this paper primarily focuses on the mast for the space station solar arrays, but the formulations and the techniques developed in this study apply to any large and flexible mast in zero gravity. Furthermore, to determine the influence on the circular frequencies, the mass moment of inertia of the mast has been incorporated into the governing equation of motion for bending. A finite element technique (MSC/NASTRAN) has been used to verify the formulation derived in this paper. Results indicate that when the mast is relatively flexible and long, the mast mass moment of inertia influences the circular frequencies.

Introduction

With the evolution of man-tended or manned spacecraft such as Space Station Freedom comes the need for generating more electrical power than for an ordinary satellite. More electrical power simply translates to having a greater number of solar arrays with larger surface areas. In order to have a large surface area solar array and yet be able to package the folded solar array in a launch vehicle, the solar arrays should be designed with a relatively large aspect ratio. Because solar arrays for manned spacecraft require a large aspect ratio, their supporting structures (preloaded masts) will be as tall as and much more flexible than the mast for an ordinary satellite. Therefore, the assumptions made to formulate the governing equation of motion for a compact solar array will not be applicable for a solar array with a large aspect ratio. Although extensive studies have been performed on preloaded mast vibrations (refs. 1 and 2), the influence of the mast mass moment of inertia has not been considered.

Our studies focused on developing the governing equation of motion for a preloaded beam, representing a typical mast, with a tip mass, representing the storage boxes of the solar cells (fig. 1.) The equation of motion for the beam was used to derive the eigen condition (characteristic equation) whose roots are the circular frequencies of the structure in question.

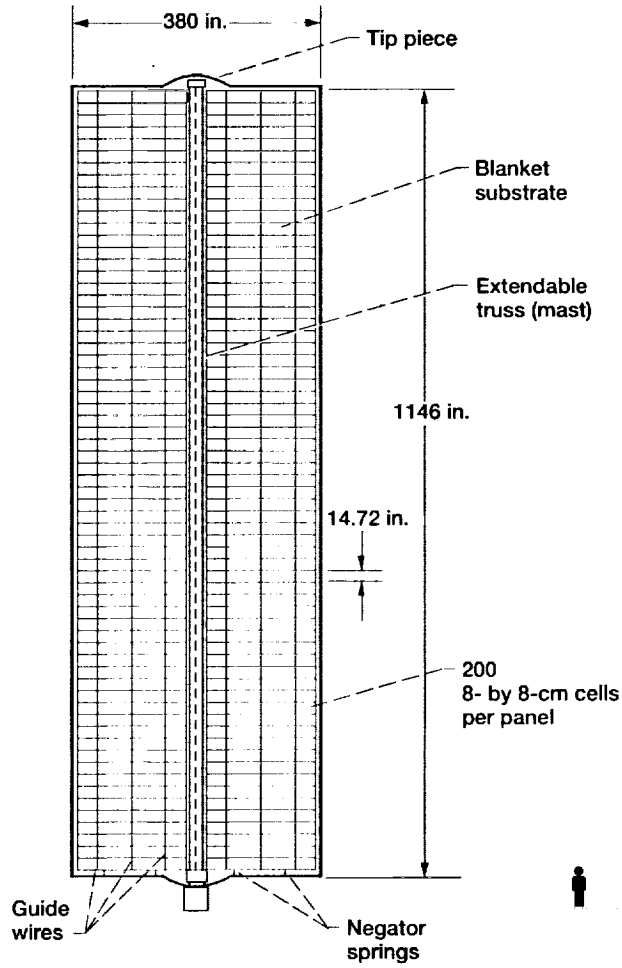

Figure 1.—Space station split blanket solar array.

The accuracy of these circular frequencies is the key in determining the forces and moments resulting from an outside excitation, such as space shuttle docking loads. The loads determined from the circular frequencies with high modal mass participation are often used to design the structure.

Symbols

C constant

EA axial stiffness

EI_{cs} flexural stiffness

F force
I moment of inertia of mast cross section
K preload parameter
K_2 tip mass preload parameter
L length of mast
M moment
M_T tip mass
m mass of mast
m' distributed mass
P preload
$\mathbf{P_D}$ component of preload in lateral direction
Q shear load
T function of time
t time
V lateral deformation as function of beam length and time
v lateral deformation as function of beam length
x distance
β frequency parameter
δ axial deflection
Θ slope of deflection
λ characteristic value
ρ mass density of the mast
ω circular frequency
∂ partial derivative

Subscript:
n nth root

Superscripts:
' differentiation with respect to length of mast
. differentiation with respect to time

Theory

The solar arrays masts are essentially bars that are subject to bending vibrations. The source of the vibrations may be the interaction of the propulsion system, and/or the shuttle docking. Since a bar is an elastic body, its mass and stiffness are distributed continuously along its length. For an elastic body the number of the generalized coordinates needed to describe the motion of the bar becomes infinite, and, as a result, the number of modes and mode shapes become infinite.

To formulate the equation of motion for and analyze a bar under a bending vibration, the following assumptions were made: (1) the material is homogeneous and isotropic, and it follows Hooke's law; (2) the continuum representing the mast is conservative, and the structural damping and viscous damping (frictional forces) are nearly zero; (3) the magnitude of displacement is small when compared to the mast length, so the sine and tangent of the angle are equal to the angle of deflection; (4) the mast has a constant cross-sectional area and constant bending stiffness along its length; and (5) the supporting spacecraft is rigid and massive when compared to the solar array mast, and the mast is fixed at its base. It is important to note that the boundary conditions for the mast are derived based on the last assumption.

The mechanism for preloading the mast (fig. 1) can be described as the tensioning of the solar array substrates by some force at their edges; a compressive force of equal magnitude will act on the mast. The substrates are tensioned to achieve flat surfaces and to increase their natural frequency to some nonzero value.

In this study the assumption has been made that the masses of the solar cell storage boxes are concentrated at only one point, the tip of the mast. Such an assumption is appropriate when analyzing the mast under a bending vibration since the storage boxes will experience the same direction and magnitude of motion during any bending mode. In contrast, one tip mass is not a valid assumption when analyzing the mast under a torsional vibration, and an appropriate mass moment inertia of the solar cell storage boxes should be considered. In summary, the continuum representing the mast is a preloaded mast that is fixed at one end and free at the other, where the tip mass is placed.

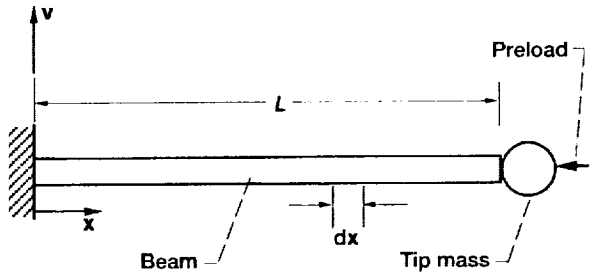

Figure 2.—Preloaded beam with a tip mass.

Governing Equation of Motion

Figure 2 shows a mast of length L, whose cross-sectional area is A and bending stiffness is EI_{cs}. The preload has a magnitude **P** in the direction shown, and the tip mass has a magnitude M_T. One very important point to be made here is that because of the mechanism for preloading the mast, the direction of the load always remains towards the root of the mast, regardless of the deflection and the mast mode shapes. This occurs because the solar cell substrates are essentially membranes and they react only to tensile loading. The magnitude of the preload remains constant, regardless of the magnitude of deflection, since the solar cell substrates contain negator

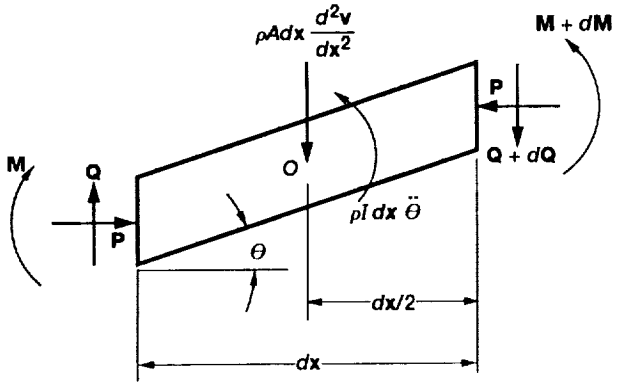

Figure 3.—Free-body diagram of a differential element of the preloaded beam.

spring mechanisms at their edges that keep the magnitude of the preload constant.

Figure 3 shows the free-body diagram of a differential element of the preloaded mast with all the forces and moments acting on its body. The sum of the loads can be expressed as follows:

$$\Sigma \mathbf{F}_{\mathbf{x}} = 0, \quad \text{which results in } \mathbf{P} = \mathbf{P} \tag{1}$$

$$\Sigma \mathbf{F}_{\mathbf{v}} = 0, \quad \text{which results in } \frac{\partial \mathbf{Q}}{\partial \mathbf{x}} = -\rho A \frac{\partial^2 \mathbf{V}}{\partial t^2} \tag{2}$$

$$\Sigma \mathbf{M}_{\mathbf{o}} = 0, \quad \text{which results in } \mathbf{Q} = \frac{\partial \mathbf{M}}{\partial \mathbf{x}} + \mathbf{P}\frac{\partial \mathbf{V}}{\partial \mathbf{x}} - \rho I \ddot{\Theta} \tag{3}$$

Using the elementary theory of strength of material gives

$$\mathbf{M} = EI_{cs} \frac{\partial^2 \mathbf{V}}{\partial \mathbf{x}^2} \tag{4}$$

and

$$\Theta = \frac{\partial \mathbf{V}}{\partial \mathbf{x}} \tag{5}$$

By differentiating equation (4) with respect to **x** once, differentiating equation (5) with respect to t twice, and then substituting the results into equation (3), we obtain

$$\mathbf{Q} = EI_{cs} \frac{\partial^3 \mathbf{V}}{\partial \mathbf{x}^3} + \mathbf{P}\frac{\partial \mathbf{V}}{\partial \mathbf{x}} - \rho I \frac{\partial}{\partial \mathbf{x}}\left(\frac{\partial^2 \mathbf{V}}{\partial t^2}\right) \tag{6}$$

Finally, differentiating equation (6) with respect to **x** and substituting it into equation (2) gives the equation of motion for a preloaded mast with a tip mass:

$$EI_{cs} \frac{\partial^4 \mathbf{V}}{\partial \mathbf{x}^4} + \mathbf{P}\frac{\partial^2 \mathbf{V}}{\partial \mathbf{x}^2} - \rho I \frac{\partial}{\partial t^2}\left(\frac{\partial^2 \mathbf{V}}{\partial \mathbf{x}^2}\right) = -\rho A \frac{\partial^2 \mathbf{V}}{\partial t^2} \tag{7}$$

Since the displacement **V** is a function of length **x** and time t, the method of separation of variables is used:

$$\mathbf{V} = f(\mathbf{x}, t) = \mathbf{v}(\mathbf{x})T(t) \tag{8}$$

For a harmonic excitation

$$T(t) = \sin \omega t \tag{9}$$

where ω is the circular frequency of motion.

Substituting equation (9) into equation (8) and then differentiating with respect to **x** and t and substituting the results into equation (7) gives the following:

$$\mathbf{v}'''' + \left(\frac{\mathbf{P} + \rho I \omega^2}{EI_{cs}}\right)\mathbf{v}'' - \left(\frac{\rho A \omega^2}{EI_{cs}}\right)\mathbf{v} = 0 \tag{10}$$

Equation (10) is similar to equation (7), but it represents the motion at any given time, since **v** is a function only of **x**.

Discussion of Terms in Equation (10)

When the preload and the mass moment of inertia are zero, equation (10) reduces to the equation of motion for a simple beam. In equation (10) the first term, **v**-9, represents the bending motion of a differential element of length $d\mathbf{x}$; the third term, $\left(\frac{\rho A \omega^2}{EI_{cs}}\right)\mathbf{v}$, represents the linear inertia of a differential element of length $d\mathbf{x}$ that opposes the motion; and the second term, $\left(\frac{\mathbf{P} + \rho I \omega^2}{EI_{cs}}\right)\mathbf{v}''$, is the contribution of the preload and the mass moment of inertia. The physical meaning of the second term can be described as follows: (1) When the mast is deformed laterally, the preload **P** tends to deform (bend) it even further, and the magnitude of this added displacement is proportional to the preload times the displacement lever arm; and (2) when the mast is deformed laterally, the angular acceleration tends to assist the bending of the mast in the same direction as the preload. It is interesting to note that the magnitude of this bending effect is influenced by the displacement **v** and by the circular frequency at which the system is vibrating. For high circular frequencies, this effect dominates the influence of preload.

General Solution

For simplicity, let us define

$$K^2 = \frac{\mathbf{P} + \rho I \omega^2}{EI_{cs}} \tag{11}$$

and

$$\beta^4 = \frac{\rho A \omega^2}{EI_{cs}} \tag{12}$$

where β is the frequency parameter (ref. 2).

Substituting equations (11) and (12) into equation (10) results in

$$\mathbf{v}'''' + K^2\mathbf{v}'' - \beta^4\mathbf{v} = 0 \tag{13}$$

Equation (13) is a fourth order ordinary differential equation with the general solution

$$\mathbf{v} = C_1 \cosh \lambda_1\mathbf{x} + C_2 \sinh \lambda_1\mathbf{x} + C_3 \cos \lambda_2\mathbf{x} + C_4 \sin \lambda_2\mathbf{x} \tag{14}$$

where

$$\lambda_1 = \sqrt{\frac{-K^2 + \sqrt{K^4 + 4\beta^4}}{2}} \tag{15}$$

and

$$\lambda_2 = \sqrt{\frac{K^2 + \sqrt{K^4 + 4\beta^4}}{2}} \tag{16}$$

The constants C_1 to C_4 can be determined from the boundary conditions and the initial condition.

At the fixed end of the mast, the displacement and the slope of the displacement are zero; thus the first two boundary conditions are

$$\mathbf{v}(0) = 0 \tag{17}$$

$$\left.\frac{d\mathbf{v}}{d\mathbf{x}}\right|_{\mathbf{x}=0} = 0 \tag{18}$$

Because the boundary condition at the free end, where the tip mass is placed, is more complex, a free-body diagram of the free end is required. Figure 4 shows the mast as loaded; in this figure, $\mathbf{P_D}$ is a component of preload whose magnitude can be determined as follows:

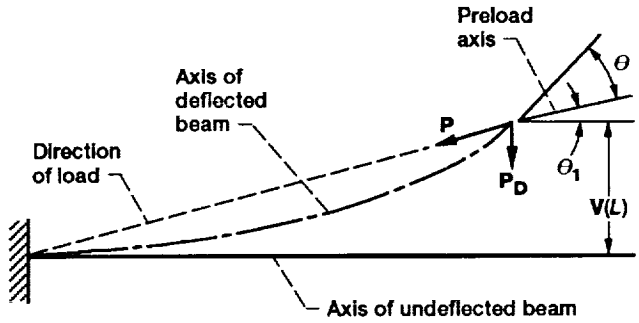

Note: For a small lateral deflection $\theta_1 = \theta = \tan(\theta) = \sin(\theta)$

Figure 4.—Deflected shape of the preloaded beam centerline.

$$\tan \Theta \cong \frac{\mathbf{V}(L)}{L - \delta} \tag{19}$$

and

$$\mathbf{P_D} = \mathbf{P} \sin \Theta \tag{20}$$

Note that when the mast is deflected, its length is shortened by some magnitude δ.

For a small deflection, $\Theta \cong \tan \Theta \cong \sin \Theta$; therefore

$$\mathbf{P_D} = \mathbf{P} \sin \Theta \cong \mathbf{P}\Theta = \mathbf{P}\frac{\mathbf{V}(L)}{L - \delta} \tag{21}$$

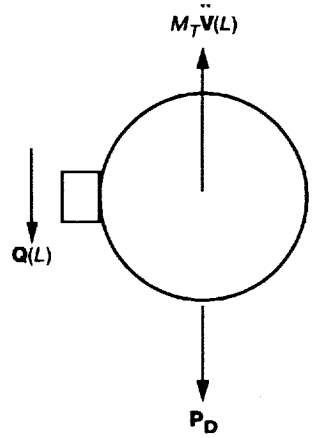

Figure 5.—Free-body diagram at free end of the preloaded beam.

where δ is the axial deflection whose magnitude is influenced by the axial preload. Its magnitude (ref. 3) is

$$\delta = \frac{\mathbf{P}L}{EA} \tag{22}$$

Substituting equation (22) into (21) gives

$$\mathbf{P_D} = \mathbf{P}\frac{\mathbf{V}(L)}{L - \frac{\mathbf{P}L}{EA}} \tag{23}$$

Figure 5 depicts the free-body diagram at the mast's free end. To eliminate the time function, the terms from equations (8) and (9) should be substituted for the terms in this free-body diagram. Summing the forces and moments at the mast free end results in

$$\mathbf{Q}(L) + \frac{\mathbf{P}\mathbf{v}(L)}{L - \frac{\mathbf{P}L}{EA}} - M_T\omega^2\mathbf{v}(L) = 0 \tag{24}$$

and

$$M(L) = EI_{cs}\left.\frac{d^2\mathbf{v}}{d\mathbf{x}^2}\right|_{\mathbf{x}=L} = 0 \tag{25}$$

Note that since the direction of the preload always remains towards the mast fixed end, the moment caused by the preload about the mast fixed end is zero.

If the mast is tall and flexible so that $EA >> \mathbf{P}L$, then equation (24) can be simplified to

$$Q(L) + \frac{\mathbf{P}\mathbf{v}(L)}{L} - M_T\omega^2\mathbf{v}(L) = 0 \tag{26}$$

Therefore, equations (25) and (26) are the boundary conditions to be used at the mast free end. Using the first two boundary conditions (eqs. (17) and (18)) results in

$$C_3 = -C_1 \tag{27}$$

and

$$C_4 = -\frac{\lambda_1}{\lambda_2}C_2 \tag{28}$$

Employing the third condition (eq. (26)) and equation (6) gives

$$\begin{aligned} C_1\Big[&\left(\lambda_1^3 + \lambda_1\lambda_2^2\right)\sinh\lambda_1 L + \left(\lambda_2 + \lambda_1^2 - \lambda_2^3\right)\sin\lambda_2 L \\ &+ K_2\left(\cosh\lambda_1 \mathrm{L} - \cos\lambda_2 L\right) \\ &+ C_2\Bigg[\left(\lambda_1^3 + \lambda_1\lambda_2^2\right)\cosh\lambda_1 L \\ &+ \left(-\lambda_2\lambda_1^2 + \lambda_2^3\right)\frac{\lambda_1}{\lambda_2}\cos\lambda_2 L \\ &+ K_2\left(\sinh\lambda_1 \mathrm{L} - \frac{\lambda_1}{\lambda_2}\sin\lambda_2 L\right)\Bigg] = 0 \end{aligned} \tag{29}$$

where

$$K_2 = \frac{M_T\omega^2 - \frac{\mathbf{P}}{L}}{EI_{cs}} \tag{30}$$

Note that the following relations, which can easily be checked, simplify equation (29): $\lambda_1\lambda_2 = \beta^2$; $\lambda_1^2 + K^2 = \lambda_2^2$; and $\lambda_2^2 - K^2 = \lambda_1^2$. Thus equation (29) becomes

$$\begin{aligned} C_1\Big[&\lambda_1\lambda_2^2\sinh\lambda_1 L - \lambda_1^2\lambda_2\sin\lambda_2 L + K_2\left(\cosh\lambda_1 L - \cos\lambda_2 L\right)\Big] \\ &+ C_2\Bigg[\lambda_1\lambda_2^2\cosh\lambda_1 L + \lambda_1^3\cos\lambda_2 L \\ &+ K_2\left(\sinh\lambda_1 L - \frac{\lambda_1}{\lambda_2}\sinh\lambda_2 L\right)\Bigg] = 0 \end{aligned} \tag{31}$$

Employing the fourth condition (eq. (25)) results in

$$\begin{aligned} &C_1\left(\lambda_1^2\cosh\lambda_1 L + \lambda_2^2\cos\lambda_2 L\right) \\ &+ C_2\left(\lambda_1^2\sinh\lambda_1 L + \lambda_1\lambda_2\sin\lambda_2 L\right) = 0 \end{aligned} \tag{32}$$

Table I. - Parameters Which Define the Idealized Solar Array Structure [ref. 4]

Length, in.	1146
Width, in.	380
Beam EI_{cy}, psi	2.85×10^{8}
Beam, psi	6.9×10^{6}
Beam weight, lb	286.5
Blanket weight, lb	766
Tip weight, lb	67
Tip inertia, lb-in.^{2}	8.06×10^{5}

Equations (31) and (32) represent an eigenvalue problem. The determinant of C_1 and C_2 must be zero, and this condition establishes the characteristics equation (having an infinite number of roots) that determines the characteristic number or frequency value. Setting the determinant of equations (31) and (32) to zero gives

$$2\beta^6 - K^2\beta^4 \sinh \lambda_1 L \sin \lambda_2 L + \beta^2\left(K^4 + 2\beta^4\right)\cosh \lambda_1 L \cos \lambda_2 L - K_2\left(\lambda_1^2 + \lambda_2^2\right) \times \left(\lambda_1 \cosh \lambda_1 L \sin \lambda_2 L - \lambda_2 \sinh \lambda_1 L \cos \lambda_2 L\right) = 0 \tag{33}$$

Equation (33) is similar to the eigen condition derived in reference 2, with some minor differences in definition of parameters. Note that all parameters in equation (33) are functions of ω, and employing the constants from table I will result in a highly nonlinear equation with an infinite number of roots.

Mode Shapes

To determine the mode shapes, the constants C_1 to C_4 should be evaluated and substituted into equation (14). The boundary conditions of the mast can provide the necessary information to evaluate any set of three constants, but the last constant can be evaluated only with the initial condition. Since we are interested in the mode shapes at any instant of time and since the last constant can have any value, depending on the initial condition, an arbitrary value of 1.0 for the last constant is assumed in this study.

Substituting equations (27) and (28) into equation (14) results in

$$\mathbf{V} = C_1\left(\cosh \lambda_1 \mathbf{x} - \cos \lambda_2 \mathbf{x}\right) + C_2\left(\sinh \lambda_1 \mathbf{x} - \frac{\lambda_1}{\lambda_2}\sin \lambda_2 \mathbf{x}\right) \tag{34}$$

Solving equation (29) for C_2 and substituting that into equation (34) yields

$$\mathbf{v} = C_1\left\{\left(\cosh \lambda_1 \mathbf{x} - \cos \lambda_2 \mathbf{x}\right) - \left[\frac{\lambda_1\lambda_2^2 \sinh \lambda_1 L - \lambda_1^2\lambda_2 \sin \lambda_2 L + K_2\left(\cosh \lambda_1 L - \cos \lambda_2 L\right)}{\lambda_1\lambda_2^2 \cosh \lambda_1 L + \lambda_1^3 \cos \lambda_2 L + K_2\left(\sinh \lambda_1 L - \frac{\lambda_1}{\lambda_2}\sin \lambda_2 L\right)}\right] \times \left(\sinh \lambda_1 \mathbf{x} - \frac{\lambda_1}{\lambda_2}\sin \lambda_2 \mathbf{x}\right)\right\} \tag{35}$$

Equation (35) is the equation of motion for individual circular frequencies. When a circular frequency obtained from equation (33) is substituted into equation (35), the mode shape for that particular frequency can be determined. Note that, as stated previously, the value for C_1 is assumed to be 1.0 prior to mode shapes determination.

When the mast is excited, it will vibrate through all frequencies; therefore its motion, which is the sum of all mode shapes, can be expressed as

$$\mathbf{v} = \sum_{n=1}^{\infty} C_n\left\{\left(\cosh \lambda_{1n} \mathbf{x} - \cos \lambda_{2n} \mathbf{x}\right) - \left[\frac{\lambda_{1n}\lambda_{2n}^2 \sinh \lambda_{1n} L - \lambda_{1n}^2\lambda_{2n} \sin \lambda_{2n} L + K_2\left(\cosh \lambda_{1n} L - \cos \lambda_{2n} L\right)}{\lambda_{1n}\lambda_{2n}^2 \cosh \lambda_{1n} L + \lambda_{1n}^3 \cos \lambda_{2n} L + K_2\left(\sinh \lambda_{1n} L - \frac{\lambda_{1n}}{\lambda_{2n}}\sin \lambda_{2n} L\right)}\right] \times \left(\sinh \lambda_{1n} \mathbf{x} - \frac{\lambda_{1n}}{\lambda_{2n}}\sin \lambda_{2n} \mathbf{x}\right)\right\} \tag{36}$$

where the subscript n refers to the nth circular frequency.

Again, it should be emphasized that equation (36) is the mode shape at any instant of time; to obtain the mode shape as function of the mast length and time, use equations (8) and (9), which yield

$$v = \sum_{n=1}^{\infty} C_n \left\{ (\cosh \lambda_{1n} x - \cos \lambda_{2n} x) - \left[\frac{\lambda_{1n}\lambda_{2n}^2 \sinh \lambda_{1n} L - \lambda_{1n}^2 \lambda_{2n} \sin \lambda_{2n} L + K_2 (\cosh \lambda_{1n} L - \cos \lambda_{2n} L)}{\lambda_{1n}\lambda_{2n}^2 \cosh \lambda_{1n} L + \lambda_{1n}^3 \cos \lambda_{2n} L + K_2 \left(\sinh \lambda_{1n} L - \frac{\lambda_{1n}}{\lambda_{2n}} \sin \lambda_{2n} L \right)} \right] \times \left(\sinh \lambda_{1n} x - \frac{\lambda_{1n}}{\lambda_{2n}} \sin \lambda_{3n} x \right) \right\} \sin \omega_n t \qquad (37)$$

where C_n is obtained by using the initial condition.

Finite Element Approach

Since the normal mode solution of MSC/NASTRAN (Version 65c) does not have the capability of predicting the normal modes of a preloaded structure in one computer run, the general solution was divided into two separate runs. First the stiffness matrix of the preloaded mast was generated by using the geometric nonlinearity of solution 64 of MSC/NASTRAN, and then the superelement normal mode, solution 63, was used to determine the modes.

Static Nonlinear and Normal Mode Solutions

The finite element model of the mast, shown in figure 6, is approximately a 100 degree-of-freedom model, which contains BEAM elements. BEAM elements are two-noded elements with the capability of deforming axially, laterally, and torsionally. For this study the torsional deformation capability of the finite element model was eliminated by constraining all the nodes from rotating about the x-direction. Also the model was forced to bend in only one direction by

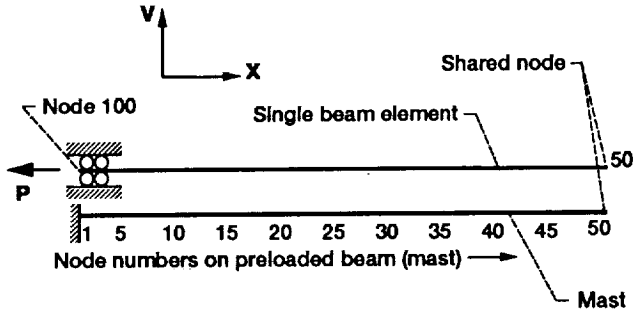

Figure 6.—A representation of the finite element model of the preloaded beam. Note: The mast and single beam element are physically at the same location, but in this figure they have been shown separately to emphasize the physics of loading. Node 50 is a shared node with a hinge.

constraining all the nodes in the z-direction. Node 1, which represents the fixed end of the mast, is constrained in all directions.

To generate the preload on the mast, and yet force the direction of the preload to remain towards the fixed end of the mast, a single BEAM element with a very large stiffness was generated, running the entire length of mast. The single BEAM element shares node 50 with the mast. The large stiffness of the single BEAM element ensures that no mode coupling will occur between the mast and the single BEAM element. The node at the other end of the single BEAM element is node 100, which has been located 0.094 in. above node 1, in the positive x-direction. The reason for this offset is that when a preload (see table I) is applied to the mast, because of the axial flexibility of the mast, the entire assembly will deform by 0.094 in. towards the negative x-direction. To enforce the motion of node 100 in the direction of the preload, a constraint in the v-direction was applied to this node. In addition, to eliminate the bending action between the single BEAM element and the mast, a hinge was placed at node 50.

Finally, the database containing the preloaded stiffness matrix of the mast was used in solution 63 to obtain the circular frequencies. The Generalized Dynamic Reduction technique was used to extract the circular frequencies.

Results

A Fortran program was developed to solve equation (33) for circular frequencies by using the Newton method. The circular frequencies from the Fortran program and the finite element model of the mast are shown in tables II to IV. In these tables the values for the mass moment of inertia and the preload vary from zero to their maximum values. The circular frequencies from equation (33) and from the finite element model of the mast are nearly identical at each mode; thus the Fortran program was verified for accuracy.

Table II. – Comparison of Frequencies Obtained From MSC/NASTRAN and Equation (33) With $I = 0$ in.^{4} and **P** = 0 [M_t = 67 lb]

Modes	Frequency, Hz	
	MSC/NASTRAN	Equation (33)
First	1.27	1.27
Second	9.07	9.07
Third	26.86	26.87

Table III. – Comparison of Frequencies Obtained From MSC/NASTRAN and Equation (33) With $I = 0$ in.^{4} and **P** = 150 lb [M_t = 67 lb]

Modes	Frequency, Hz	
	MSC/NASTRAN	Equation (33)
First	1.25	1.25
Second	8.88	8.90
Third	26.44	26.71

Table IV. – Comparison of Frequencies Obtained From MSC/NASTRAN and Equation (33) With $I = 38$ in.^{4} and **P** = 150 lb [M_t = 67 lb]

Modes	Frequency, Hz	
	MSC/NASTRAN	Equation (33)
First	1.25	1.25
Second	8.88	8.90
Third	26.44	26.67

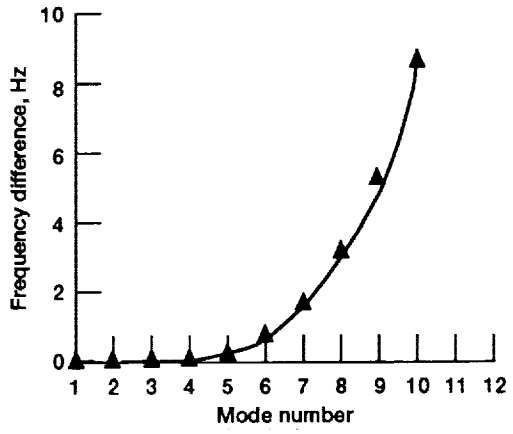

Figure 7.—Frequency differences from table V as a function of mode number.

Table V. – Comparison of Frequencies Obtained From Equation (33) for Two Cases: $I = 0$, and $I = 38$ in.^{4} [**P** = 150 lb and M_t = 67 lb]

Mode number	Frequency, Hz		
	I = 38 in.^{4}	I = 0 in.^{4}	Difference
1	1.2455	1.2455	0
2	8.8963	8.9005	.0042
3	26.6714	26.7064	.0350
4	54.1339	54.2774	.1435
5	91.3582	91.7687	.4105
6	138.2606	139.2063	.9457
7	194.7165	196.603	1.8865
8	160.5686	263.9654	3.3968
9	335.6321	341.2965	5.6644
10	419.6985	428.5986	8.9001

To determine the influence of the mast mass moment of inertia on circular frequencies, the first 10 circular frequencies were extracted and tabulated in table V for 2 mass moments of inertia input to the Fortran program, namely, $I = 0$ in.^{4} and $I = 38$ in.^{4} The differences between these circular frequencies are shown in table V and plotted in figure 7; note that as the mode number increases, the influence of the mast mass moment of inertia becomes more apparent. The relationship between the mode number and the frequency difference in figure 7 appears to be that of a second order polynomial. MSC/NASTRAN was not included in the study performed for table V, since for higher frequencies the mast finite element model demands higher fidelity. This model will need to be further refined.

To incorporate the influence of the mass moment of inertia into the finite element model of the mast, the following methods were investigated: (1) the mass moment of inertia of each BEAM element of the mast was calculated and applied to the BEAM property card as the nonstructural mass moment of inertia; and (2) the mass moments of inertia of the BEAM elements (calculated in step 1) were applied to concentrated mass elements (CONM2), and these elements were placed on nodes 1 to 50. As expected, the circular frequencies from the finite element model of the mast were not affected at all, because the influence of the mass moment of inertia has not been included in the Euler beam formulation.

For a cantilevered beam such as the structure of the mast, where most of modal energy is stored in its first few modes, it is crucial to predict the first few circular frequencies accurately. The reason for this is that the dynamic loads are generally proportional to the inverse of the circular frequencies. As can be observed in tables II and IV, the frequencies obtained from MSC/NASTRAN are accurate. However as the demand for higher circular frequencies grows, MSC/NASTRAN becomes less accurate.

Conclusions

From the work reported herein, the following conclusions may be drawn:

1. Equation (33) is the eigen condition for the characteristic equation of the preloaded mast with a tip mass whose infinite number of roots are the circular frequencies of the structure.

2. According to our formulations and analyses, MSC/NASTRAN is accurate for predicting the bending circular frequencies of masts as long as the influence of the mass moment of inertia of the beam is small.

Lewis Research Center
National Aeronautics and Space Administration
Cleveland, Ohio, February 3, 1992

References

1. Hughes, F.C. and Garg S.C.: Dynamics of Large Flexible Solar Arrays and Application to Spacecraft Attitude Control System Design, UTIAS Report No. 179, University of Toronto, Canada, 1973 (avail. NTIS).
2. Shaker, F.J.: Effect of Axial Load on Mode Shapes and Frequencies of Beams, NASA TN D–8109, 1975.
3. Juvinall, R.C.: Engineering Considerations of Stress, Strain, and Strength, McGraw-Hill, New York, 1967.
4. Carrney, K.S.; and Shaker F.C.: Free-Vibration Characteristics and Correlation of a Space Station Split-Blanket Solar Array, NASA TM–101452, 1989.

Bibliography

Flugge, W.: Handbook of Engineering Mechanics, McGraw-Hill, New York, 1962.

"MSC/NASTRAN Application Manual, The MacNeal-Schwendler Corporation, Los Angeles, CA, 1984."

Spiegel, M.R.: Schaum's Outline of Theory and Problems of Fourier Analysis, with Applications to Boundary Value Problems, McGraw-Hill, New York, 1974.

Timoshenko, S.; Young, D.H.; and Weaver, W.: Vibration Problems in Engineering, Wiley, New York, 1974.

REPORT DOCUMENTATION PAGE

Form Approved
OMB No. 0704-0188

1. AGENCY USE ONLY (*Leave blank*)	2. REPORT DATE	3. REPORT TYPE AND DATES COVERED
	August 1992	Technical Paper

4. TITLE AND SUBTITLE
Influence of Mass Moment of Inertia on Normal Modes of Preloaded Solar Array Mast

5. FUNDING NUMBERS
WU-474-46-10

6. AUTHOR(S)
Sasan C. Armand and Paul Lin

7. PERFORMING ORGANIZATION NAME(S) AND ADDRESS(ES)
National Aeronautics and Space Administration
Lewis Research Center
Cleveland, Ohio 44135-3191

8. PERFORMING ORGANIZATION REPORT NUMBER
E-6847

9. SPONSORING/MONITORING AGENCY NAMES(S) AND ADDRESS(ES)
National Aeronautics and Space Administration
Washington, D.C. 20546-0001

10. SPONSORING/MONITORING AGENCY REPORT NUMBER
NASA TP-3273

11. SUPPLEMENTARY NOTES
Sasan C. Armand, NASA Lewis Research Center; Paul Lin, Cleveland State University, Cleveland, Ohio 44115. Responsible person, Sasan C. Armand, (216) 433-6734.

12a. DISTRIBUTION/AVAILABILITY STATEMENT
Unclassified - Unlimited
Subject Categories 39 and 37

12b. DISTRIBUTION CODE

13. ABSTRACT (*Maximum 200 words*)

Earth-orbiting spacecraft often contain solar arrays or antennas supported by a preloaded mast. Because of weight and cost considerations, the structures supporting the spacecraft appendages are extremely light and flexible; therefore, it is vital to investigate the influence of all physical and structural parameters that may influence the dynamic behavior of the overall structure. The study reported in this paper primarily focuses on the mast for the space station solar arrays, but the formulations and the techniques developed in this study apply to any large and flexible mast in zero gravity. Furthermore, to determine the influence on the circular frequencies, the mass moment of inertia of the mast has been incorporated into the governing equation of motion for bending. A finite element technique (MSC/NASTRAN) has been used to verify the formulation derived in this paper. Results indicate that when the mast is relatively flexible and long, the mast mass moment of inertia influences the circular frequencies.

14. SUBJECT TERMS
Dynamics of preloaded beams

15. NUMBER OF PAGES
12

16. PRICE CODE
A03

17. SECURITY CLASSIFICATION OF REPORT	18. SECURITY CLASSIFICATION OF THIS PAGE	19. SECURITY CLASSIFICATION OF ABSTRACT	20. LIMITATION OF ABSTRACT
Unclassified	Unclassified	Unclassified	

NSN 7540-01-280-5500

Standard Form 298 (Rev. 2-89)
Prescribed by ANSI Std. Z39-18
298-102

NASA-Langley, 1992